Journal of Alloys and Compounds 509 (2011) L314–L317

Contents lists available at ScienceDirect

Journal of Alloys and Compounds

journal homepage: www.elsevier.com/locate/jallcom

Letter

Sintering effect on electrical properties of $ZnO–V_2O_5–MnO_2–Nb_2O_5$ ceramics

Choon-W. Nahm*

Semiconductor Ceramics Laboratory, Department of Electrical Engineering, Dongeui University, Busan 614-714, Republic of Korea

HIGHLIGHTS

►$ZnO-V_2O_5$-based varistor ceramics for low sintering temperature (900 °C). ►$ZnO-V_2O_5-MnO_2-Nb_2O_5$ (ZVMN) varistor ceramics exhibited good varistor properties, with high nonlinear coefficient (50) at 900 °C in sintering temperature. ►ZVMN varistor ceramics are a new basic composition for low sintering temperature.

ARTICLE INFO

Article history:
Received 28 May 2011
Received in revised form 11 June 2011
Accepted 14 June 2011
Available online 21 June 2011

Keywords:
Ceramics
Sintering
Electrical properties
Varistors

ABSTRACT

The microstructure and electrical properties of quaternary $ZnO–V_2O_5–MnO_2–Nb_2O_5$ ceramics were investigated at different sintering temperature (875–950 °C). The average grain size increased from 4.4 μm to 9.6 μm with increasing sintering temperature. The breakdown field decreased from 6991 V/cm to 943 V/cm with increasing sintering temperature. Proper sintering for quaternary $ZnO–V_2O_5–MnO_2–Nb_2O_5$ ceramics led to surprisingly high nonlinear coefficient (50). The donor concentration increased from 3.33×10^{17} cm^{-3} to 7.64×10^{17} cm^{-3} with increasing sintering temperature and the barrier height exhibited the maximum value (1.07 eV) at 900 °C.

1. Introduction

Zinc oxide (ZnO) is a useful material that possesses wide range of applications for gas sensor, optical devices, and electrical devices, etc. A pure zinc oxide ceramics sintered is a polycrystalline ceramic semiconductors and it exhibits linear properties even at any sintering condition. However, the sintered pellet of zinc oxide added with specific additives can exhibit strong nonlinear properties, which give rise to abrupt decrease of impedance at critical voltage in accordance with increasing voltage, so-called ZnO-nonlinear resistor (ZNR) [1,2]. The sintering process gives rise to a microstructure, which consist of semiconducting n-type ZnO grains surrounded by very thin insulating intergranular layers. Each ZnO grain acts as if it has a semiconductor junction at the grain boundary. Since nonlinear electrical behavior occurs at each boundary, the doped ZnO ceramics can be considered as a multi-junction device composed of many series and parallel connection of grain boundaries. Owing to highly nonlinear properties, the ZNR has been extensively used in the field of circuit overvoltage protection, with application ranging from a few volts in electronic circuits to millions of volts in electric power systems [3,4]. In general, ZNR cannot exhibit a nonlinear behavior without adding heavy elements with large ionic radii, such as Bi and Pr. Commercial Bi_2O_3- and Pr_6O_{11}-based ZNR cannot be co-fired with a silver inner-electrode (m.p. 961 °C) in a multilayered chip component because of their high sintering temperature above 1000 °C. The $ZnO–V_2O_5$-based ceramics can be sintered at a relatively low temperature of approximately 900 °C [5]. This is important for multilayer chip component applications, because it can be co-sintered with a silver inner-electrode without using expensive Pd or Pt, compared with commercial Bi_2O_3- and Pr_6O_{11}-based ceramics. A study of $ZnO–V_2O_5$-based ceramics is yet in its early stages in many points [6–10]. The $ZnO–V_2O_5$-based ceramics requires specific additives and sintering process in order to have higher nonlinear properties [11–17]. Therefore, it is very important to investigate the effects of sintering process on electrical properties for the varistor ceramics with specified composition. The additives of MnO_2 and Nb_2O_5 are reported to improve the varistor properties in the $ZnO–V_2O_5$ ceramics [11,13]. In this study, the electrical properties of quaternary $ZnO–V_2O_5–MnO_2–Nb_2O_5$ (ZVMN) ceramics with sintering were investigated and surprisingly high nonlinear coefficient (α) were obtained by proper sintering.

2. Experimental procedure

Reagent-grade raw materials were prepared in the proportions of quaternary composition expression, such as 97.4 mol% ZnO + 0.5 mol% V_2O_5 + 2.0 mol% MnO_2 + 0.1 mol% Nb_2O_5. Raw materials were mixed by ball milling with zirconia

* Tel.: +82 51 890 1669; fax: +82 51 890 1664.
E-mail address: cwnahm@deu.ac.kr

0925-8388/$ – see front matter © 2011 Elsevier B.V. All rights reserved.
doi:10.1016/j.jallcom.2011.06.065

balls and acetone in a polypropylene bottle for 24 h. The mixture was dried at 120 °C for 12 h. The dried mixture mixed into container with acetone and 0.8 wt% polyvinyl butyral (PVB) binder of powder weight. After drying, the mixture was granulated by sieving 100-mesh screen to produce starting powder. The powder was uniaxially pressed into discs of 10 mm in diameter and 1.5 mm in thickness at a pressure of 100 MPa. The discs were covered with raw powder in alumina crucible, sintered at four fixed sintering temperatures (875 °C, 900 °C, 925 °C, and 950 °C) in air for 3 h, and furnace-cooled to room temperature. The final samples were about 8 mm in diameter and 1.0 mm in thickness. Silver paste was coated on both faces of the samples and the electrodes were formed by heating it at 550 °C for 10 min. The electrodes were 5 mm in diameter.

The surface microstructure was examined by a field emission scanning electron microscope (FESEM, Quanta 200, Czech). The average grain size (d) was determined by the linear intercept method [18]. The crystalline phases were identified by X-ray diffractometer (XRD, X′pert-PRO MPD, Netherland) with CuK_α radiation. The sintered density (ρ) was measured using a density determination kit (238490) attached to balance (Mettler AG 245, Switzerland).

The breakdown field (E_B) was measured at a current density of 1.0 mA cm^{-2} and the leakage current density (J_L) was measured at 0.80E_B. In addition, the non-ohmic coefficient (α) was determined from $\alpha = 1/(\log E_2 - \log E_1)$, where E_1 and E_2 are the electric fields corresponding to 1.0 mA cm^{-2} and 10 mA cm^{-2}, respectively.

The capacitance–voltage (C–V) characteristics of the samples were measured at 1 kHz using an RLC meter (QuadTech 7600, USA) and an electrometer (Keithley 617, USA). The donor density (N_d) and the barrier height (Φ_b) were determined by the equation $(1/C_b - 1/2\,C_{bo})^2 = 2(\Phi_b + V_{gb})/q\varepsilon N_d$ [19], where C_b is the capacitance per unit area of a grain boundary, C_{bo} is the value of C_b when $V_{gb} = 0$, V_{gb} is the applied voltage per grain boundary, q is the electronic charge, ε is the permittivity of ZnO ($\varepsilon = 8.5\varepsilon_o$). The density of interface states (N_t) at the grain boundary was determined by the equation: $N_t = (2\varepsilon N_d \Phi_b/q)^{1/2}$ [19].

3. Results and discussion

Fig. 1 shows the SEM micrographs of the samples for different sintering temperatures. It can be easily seen that the grain structure is very homogeneously distributed and the grain boundaries are clear throughout all the ceramics, compared with existing reported literature [5–11]. The average grain size of the samples increased from 4.4 μm to 9.6 μm with the increase of sintering temperature. ZnO grains could probably grow rapidly in the presence of a rich liquid phases related to V_2O_5 because the melting point of V_2O_5 is 690 °C. The sintered density of the samples decreased from 5.52 g cm^{-3} to 5.44 g cm^{-3} corresponding to 95.5–94.1% of the theoretical density (TD) (pure ZnO, TD = 5.78 g cm^{-3}) with the increase of sintering temperature. It is assumed that the decrease of sintered density is attributed to the volatility of the V-species for V_2O_5 with low melting point.

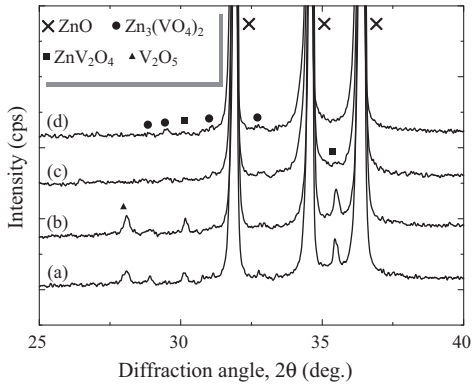

Fig. 2. XRD patterns of the samples for different sintering temperatures: (a) 875 °C, (b) 900 °C, (c) 925 °C, and (d) 950 °C.

The XRD patterns of the samples for different sintering temperatures are shown in Fig. 2. These patterns revealed the presence of $Zn_3(VO_4)_2$ and ZnV_2O_4 as minor secondary phases, which act as liquid-phase sintering aids, in addition to a major phase of hexagonal ZnO [14]. The detailed microstructure parameters are summarized in Table 1.

Fig. 3 shows the electric field–current density (E–J) characteristics of the samples for different sintering temperatures. The varistor properties are characterized by non-ohmic conduction in the E–J characteristics. The curves are clearly divided into two regions: one is an ohmic region with extremely high impedance before breakdown field and another is a non-ohmic region with extremely low impedance after breakdown field. The sharper the knee of the

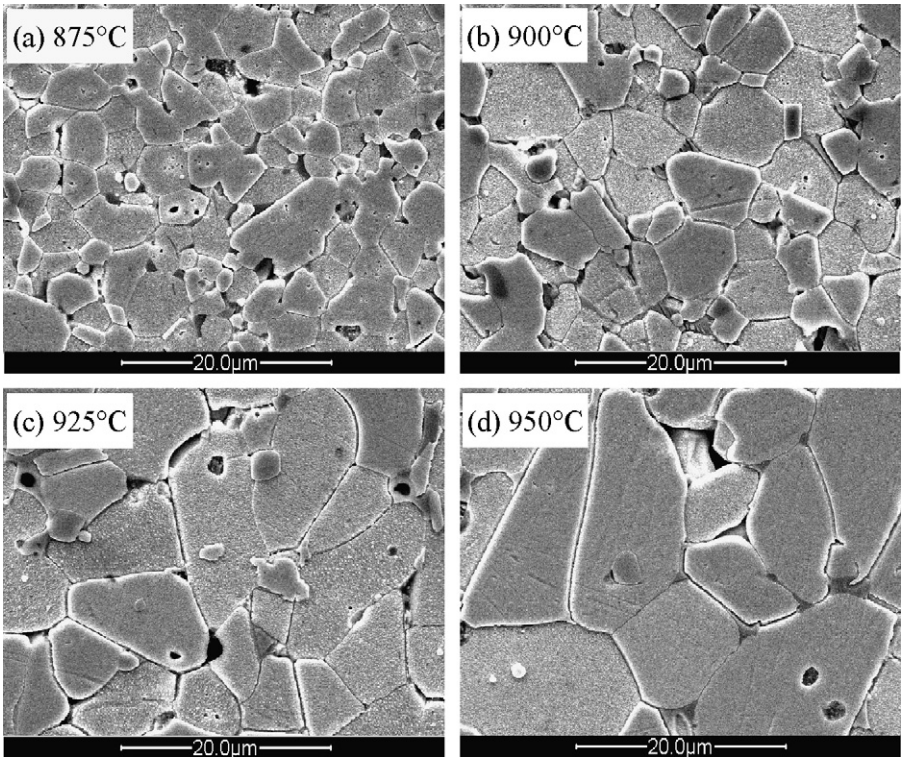

Fig. 1. SEM micrographs of the samples for different sintering temperatures.

Table 1
Microstructure, *V–I*, and *C–V* characteristic parameters of the samples for different sintering temperatures.

Sintering temp. (°C)	d (μm)	ρ (g/cm^3)	E_B (V/cm)	v_{gb} (V/gb)	α	J_L (μA/cm^2)	N_d (10^{17} cm^{-3})	Φ_b (eV)	N_t (10^{12} cm^{-2})
875	4.4	5.52	6991	3.1	44	201.3	3.33	0.95	1.73
900	5.5	5.51	4800	2.6	50	94.9	4.30	1.07	2.08
925	7.2	5.46	2241	1.6	38	25.8	6.10	0.72	2.03
950	9.6	5.44	943	0.9	25	173.7	7.64	0.54	1.98

curves between the two regions, the better the varistor properties. It can be seen from curve shapes that the sintering temperature has a significant effect on the varistor properties. The *E–J* characteristic parameters are listed in Table 1.

The breakdown field (E_B) linearly decreased from 6991 V cm^{-1} to 943 V cm^{-1} with increasing sintering temperature. The behavior of E_B in accordance with sintering temperatures can be explained by the following expression: $E_B = v_b/d$, where d is the grain size and v_b is the breakdown voltage per grain boundaries. This expression indicated that the d and v_b values directly determine E_B. Therefore, the decrease of E_B in accordance with increasing sintering temperature is attributed to the increase of the average ZnO grain size and the decrease of breakdown voltage per grain boundaries. The nonlinear coefficient (α) also linearly increased from 44 to 50 with increasing sintering temperature up to 900 °C. This is a maximum value in the quaternary ZnO-based varistors reported until now. However, further increase in sintering temperature caused α to decrease to 25 at 950 °C. This will be tuning point in the ZnO–V_2O_5-based varistor development of high performance as a new composition. As a result, it can be seen that the sintering temperature has a significant effect on the nonlinear properties in the light of the α variation. The behavior of α in accordance with sintering temperatures temperature can be related to the variation of the Schottky barrier height according to the variation of the electronic states at the grain boundaries. The sintering temperature will vary the density of interface states with the transport of the defect ions toward the grain boundary and will be more active grain boundaries. Therefore, the decrease of α in accordance with increasing sintering temperature is attributed to the decrease of potential barrier height at the grain boundaries. The current density (J_L) exhibited very high values compared with other varistor ceramics and this is a problem to work out in the near future.

Fig. 4 shows the capacitance–voltage (*C–V*) characteristics of the samples for different sintering temperatures. The detailed *C–V* characteristic parameters, such as donor concentration (N_d), barrier height (Φ_b), and density of interface states (N_t) are summarized in Table 1. The N_d increased from 3.33×10^{17} cm^{-3} to 7.64×10^{17} cm^{-3} in accordance with increasing sintering temperatures. The increase of N_d value is assumed to be due to the

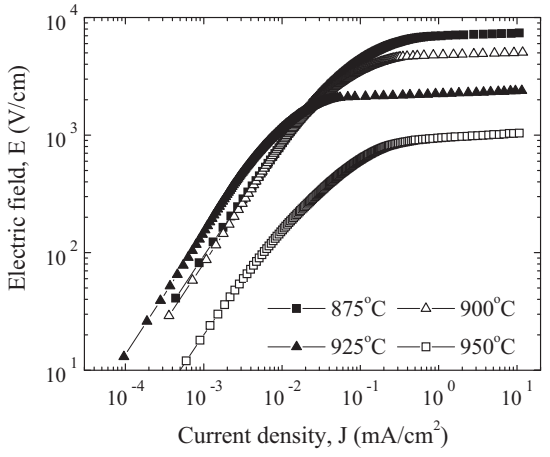

Fig. 3. *E–J* characteristics of the samples for different sintering temperatures.

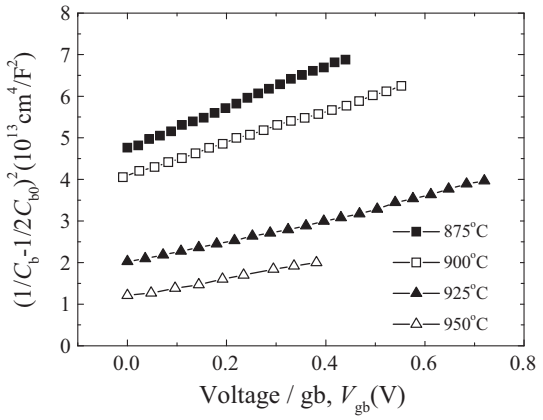

Fig. 4. *C–V* characteristics of the samples for different sintering temperatures.

dissociation of zinc oxide in the following chemical reaction expression, $ZnO \rightarrow Zn_i^x + (1/2)O_2$, $Zn_i^x \rightarrow Zn_i^{\cdot} + e'$, where Zn_i^x is a neutral zinc of interstitial site, $Zn_i^{\cdot}$ is a positively charged zinc ion of interstitial site. It is assumed that the enhancement of the donor density results from a lot of dissociation quantities of zinc oxide when the sintering temperature increases [20]. The barrier height (Φ_b) at the grain boundaries increased from 0.95 eV to 1.07 eV with increasing sintering temperature up to 900 °C. However, further increase in sintering temperature caused Φ_b to decrease to 0.54 eV at 950 °C. The behavior of Φ_b in accordance with sintering temperatures exhibited to accord to the behavior of N_t at the grain boundaries. The behavior of Φ_b and N_t coincides with the behavior of α in the *E–J* characteristics. Really, the higher barrier gives rise to the higher nonlinear coefficient.

4. Conclusions

The microstructure and electrical properties of quaternary ZnO–V_2O_5–MnO_2–Nb_2O_5 ceramics were investigated at different sintering temperature. The average grain size increased from 4.4 μm to 9.6 μm with increasing sintering temperature. The breakdown field decreased from 6991 V/cm to 943 V/cm with increasing sintering temperature. The quaternary ceramics sintered at 900 °C exhibited surprisingly high nonlinear coefficient of 50. The donor concentration increased from 3.33×10^{17} cm^{-3} to 7.64×10^{17} cm^{-3} with increasing sintering temperature and the barrier height exhibited the maximum value (1.07 eV) at 900 °C. Conclusively, it is believed that quaternary ZnO–V_2O_5–MnO_2–Nb_2O_5 ceramics will be used as a new basic composition in the development of advanced varistors.

References

[1] M. Matsuoka, Jpn. J. Appl. Phys. 10 (1971) 736.
[2] H.R. Pilipp, L.M. Levinson, J. Appl. Phys. 46 (1976) 1332.
[3] L.M. Levinson, H.R. Philipp, Am. Ceram. Soc. Bull. 65 (1986) 639.
[4] T.K. Gupta, J. Am. Ceram. Soc. 73 (1990) 1817.
[5] J.-K. Tsai, T.-B.J. Wu, Appl. Phys. 76 (1994) 4817.
[6] J.-K. Tsai, T.-B. Wu, Mater. Lett. 26 (1996) 199.
[7] C.T. Kuo, C.S. Chen, I.-N. Lin, J. Am. Ceram. Soc. 81 (1998) 2942.
[8] H.-H. Hng, K.M. Knowles, J. Am. Ceram. Soc. 83 (2000) 2455.
[9] H.-H. Hng, P.L. Chan, Mater. Chem. Phys. 75 (2002) 61.

[10] H.-H. Hng, L. Halim, Mater. Lett. 57 (2003) 1411.
[11] C.-W. Nahm, J. Mater. Sci. 42 (2007) 8370.
[12] C.-W. Nahm, Ceram. Int. 35 (2010) 3435.
[13] C.-W. Nahm, J. Alloy Compd. 490 (2010) L52.
[14] C.-W. Nahm, Ceram. Int. 36 (2010) 1109.
[15] C.-W. Nahm, Mater. Lett. 64 (2010) 830.
[16] C.-W. Nahm, J. Mater. Sci.: Mater. Electron. 21 (2010) 540.
[17] C.-W. Nahm, J. Mater. Sci.: Mater. Electron. 22 (2011) 444.
[18] J.C. Wurst, J.A. Nelson, J. Am. Ceram. Soc. 55 (1972) 109.
[19] M. Mukae, K. Tsuda, I. Nagasawa, J. Appl. Phys. 50 (1979) 4475.
[20] M.F. Yan, A.H. Heuer, Additives Interfaces in Electronic Ceramics, Am. Ceram. Soc., Columbus, OH, 1983, p. 80.